High Pressure Research: An International Journal
Publication details, including instructions for authors and subscription information:
http://www.tandfonline.com/loi/ghpr20

Thermal evolution of the metastable r8 and bc8 polymorphs of silicon

Bianca Haberl[a], Malcolm Guthrie[b], Stanislav V. Sinogeikin[c], Guoyin Shen[c], James S. Williams[a] & Jodie E. Bradby[a]

[a] Department of Electronic Materials Engineering, Research School of Physics and Engineering, The Australian National University, Canberra, ACT 0200, Australia

[b] Geophysical Laboratory, Carnegie Institution for Science, Washington, DC 20015, USA

[c] High Pressure Collaborative Access Team (HPCAT), Geophysical Laboratory, Carnegie Institution of Washington, Argonne, IL 60439, USA

Published online: 28 Jan 2015.

To cite this article: Bianca Haberl, Malcolm Guthrie, Stanislav V. Sinogeikin, Guoyin Shen, James S. Williams & Jodie E. Bradby (2015): Thermal evolution of the metastable r8 and bc8 polymorphs of silicon, High Pressure Research: An International Journal, DOI: 10.1080/08957959.2014.1003555

To link to this article: http://dx.doi.org/10.1080/08957959.2014.1003555

High Pressure Research, 2015
http://dx.doi.org/10.1080/08957959.2014.1003555

Taylor & Francis
Taylor & Francis Group

Thermal evolution of the metastable r8 and bc8 polymorphs of silicon

Bianca Haberl[a*†], Malcolm Guthrie[b‡], Stanislav V. Sinogeikin[c], Guoyin Shen[c], James S. Williams[a] and Jodie E. Bradby[a]

[a]*Department of Electronic Materials Engineering, Research School of Physics and Engineering, The Australian National University, Canberra, ACT 0200, Australia;* [b]*Geophysical Laboratory, Carnegie Institution for Science, Washington, DC 20015, USA;* [c]*High Pressure Collaborative Access Team (HPCAT), Geophysical Laboratory, Carnegie Institution of Washington, Argonne, IL 60439, USA*

(*Received 24 August 2014; final version received 24 December 2014*)

The kinetics of two metastable polymorphs of silicon under thermal annealing was investigated. These phases with body-centered cubic bc8 and rhombohedral r8 structures can be formed upon pressure release from metallic silicon. In this study, these metastable polymorphs were formed by two different methods, via point loading and in a diamond anvil cell (DAC). Upon thermal annealing different transition pathways were detected. In the point loading case, the previously reported Si-XIII formed and was confirmed as a new phase with an as-yet-unidentified structure. In the DAC case, bc8-Si transformed to the hexagonal-diamond structure at elevated pressure, consistent with previous studies at ambient pressure. In contrast, r8-Si transformed directly to diamond-cubic Si at a temperature of 255°C. These data were used to construct diagrams of the metastability regimes of the polymorphs formed in a DAC and may prove useful for potential technological applications of these metastable polymorphs.

Keywords: pressure-induced transitions; metastable polymorphs; silicon; *in situ* annealing

1. Introduction

The high pressure behavior of the elemental semiconductor silicon has attracted wide interest over the last 50 years and 13 different crystalline structures have been discovered.[1–10] This extensive polymorphism is clearly of fundamental interest, but may also be of technological interest. Namely, the significant effects of kinetic barriers in the Si system allow for the formation of several polymorphs that can be metastably recovered and possess altered electronic structures compared to the parent Si.[11,12] In particular, nanoparticles of the bc8 polymorph have recently been predicted as highly beneficial for photovoltaics, since they are expected to have the small band gap necessary for efficient multiple excitation generation (a new paradigm for more efficient solar cells).[13] Hence, synthesis of this polymorph in the required nanoparticle size and purity would be of technological interest. Similarly, improved photovoltaic properties

*Corresponding author. Email: bianca.haberl@gmail.com
†Present affiliation: Chemical and Engineering Materials Division, Oak Ridge National Laboratory, Oak Ridge, TN 37831, USA.
‡Present affiliation: European Spallation Source, SE-221 00 Lund, Sweden.

have also been calculated for another of the known metastable structures, the r8 phase.[14,15] This phase has been predicted to be a narrower band gap material with a higher carrier mobility compared to dc-Si and to have significantly improved absorption properties over the solar spectrum.[14,15] Thus, synthesis of this polymorph in a manner that yields sufficient volume and stability at ambient pressure and temperature is a current research focus.

Moreover, several further Si structures with potentially useful properties have been predicted, but not yet observed experimentally. For example, two possible phases, st12 and *Ibam*, may be good candidates for superconductive polymorphs of Si.[15,16] Similarly, a significant number of possible Si structures have been calculated that may possess improved photovoltaic properties such as a direct band gap.[17,18] Thus, the possible formation of these polymorphs makes the exploration of the metastable regime of Si even more interesting. Finally, additional Si phases with unidentified structures have been reported experimentally,[9,10,19] but their electronic properties and technological potential are unknown. Hence significant interest in this metastable regime exists, but with many remaining open questions.

The pressure-induced polymorphism of Si has been explored using the 'traditional' high pressure tools of opposed anvil devices, namely diamond anvil cells (DACs) [5–8] and supported taper apparati,[1,20] but also by point loading using diamond indentation tips.[9,10,21–24] Under pressure in a DAC the standard diamond-cubic (dc)-Si (space group $Fd\bar{3}m$) transforms into a metallic phase at 11.3 GPa.[1,20] This phase exhibits the white tin (β-Sn) structure with the space group $I4_1/amd$ and is 22% more dense than dc-Si.[1] Upon further compression to 13.2 GPa an orthorhombic phase with space group *Imma* is formed,[6] followed by the simple hexagonal (sh) phase (space group $P6/mmm$) at 15.6 GPa.[25] This phase in turn transforms into another orthorhombic structure (space group *Cmca*) at 38 GPa.[8] At 42 GPa, the hexagonal close-packed phase (space group $P6_3/mmc$) is nucleated, which remains stable until 79 GPa. Here it transforms into the face-centered cubic phase (space group $Fm\bar{3}m$). This phase persists to 248 GPa, the highest pressure probed to date.[26] These metal–metal transitions are reversible under standard unloading conditions, but the (β-Sn)-Si to dc-Si transition is not and instead the metastable structures are nucleated.

Upon pressure release from (β-Sn)-Si the rhombohedral (r8) phase with space group $R\bar{3}$ is reported to form at 9 GPa.[7] As pressure is decreased, a reversible transition to the body-centered cubic (bc8) structure with space group $Ia\bar{3}$ follows at 2.8 GPa.[7] The bc8 phase has been shown, experimentally and theoretically, to be a semimetal.[11,15] Two further tetragonal polymorphs with unassigned atomic positions, Si-VIII (space group $P4_12_12$) and Si-IX (space group $P4_22$), have been reported upon rapid unloading from metallic phases.[19] Interestingly, the r8 and bc8 metastable polymorphs can also be formed through pressure release from metallic Si when using point loading (*i.e.* indentation loading).[23,27] Raman spectroscopy confirms that a mixture of the r8 and bc8 phases[2] is present after final pressure release.[10,23,28] Electrical measurements on this bc8/r8-Si mixture have recently suggested that the material created by point loading is indeed a semiconductor, can be doped at room temperature [12] and can be exploited for room temperature maskless electrical patterning.[29,30]

These polymorphs are not stable Si structures and heat will transform them to the dc structure. Little work has been done, however, on the thermal stability and thermal evolution of these metastable phases. Indeed, even the pathway of the transition from bc8-Si and r8-Si to dc-Si is not fully established and different intermediate phases have been reported as summarized in a schematic in Figure 1. For example, at ambient pressure bc8-Si undergoes an irreversible transition to the lonsdaleite/hexagonal-diamond (hd) structure (space group $P6_3/mmc$) at 200°C.[2,4,31] This polymorph is a semiconductor similar to dc-Si.[11,15] Interestingly, it is unknown into which phase hd-Si transforms upon compression, into another metastable polymorph or straight into (β-Sn)-Si for example. It is known, however, that upon further annealing to $\sim$ 750°C hd-Si transforms back to the stable dc-Si.[31] This is very different if the bc8/r8

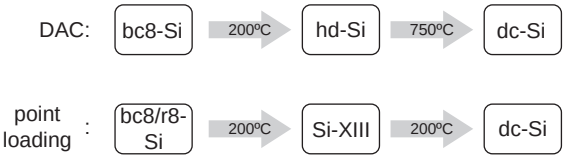

Figure 1. Schematic of the temperature-induced transition pathways at ambient pressure of bc8-Si made in a DAC and the bc8/r8-Si made via point loading as reported in the literature.[2,4,9,10,31] (See text for further details.)

phases are made through point loading. Instead of forming the hd structure, a new intermediate structure is observed at 200°C, the so-called Si-XIII.[9,10,32] The existence of Si-XIII is detected from Raman spectra, but its crystal structure remains unknown. Upon further annealing at 200°C for ∼1 week dc-Si is eventually regained, but it is not clear if hd-Si is formed as an additional intermediate phase.[10] Thus, only *ex situ* studies at ambient pressure have been performed on bc8-Si and r8-Si, although only *in situ* studies can enable the full determination of these transition pathways and the possible identification of new phases.

Therefore, in this work the thermal evolution of pressurized bc8-Si and r8-Si and the resulting phases are investigated in depth. Firstly, a mixture of bc8/r8-Si made by point loading is annealed to form Si-XIII and the transformed volume is studied using electron diffraction. Secondly, bc8-Si and r8-Si made in a DAC are annealed *in situ* while pressurized. In this latter case, the evolution of these polymorphs is followed using *in situ* synchrotron X-ray diffraction (XRD). Two additional DAC experiments on hd-Si and mixed bc8-Si and r8-Si were performed to confirm metastable transition pathways. Thus, this study yields significant new insights into the metastable regime of Si.

2. Known silicon polymorphs

In this study, several known polymorphs of Si are observed, namely dc-Si, hd-Si, bc8-Si, r8-Si, (β-Sn)-Si and also sh-Si in addition to an unknown structure, the so-called Si-XIII. The space groups and lattice parameters of the known structures are summarized in Table 1. Since these phases are structurally related to each other and indeed transform into one other, many of them exhibit overlapping d-spacings. For clarity, therefore, the lattice planes and corresponding d-spacings are calculated after Table 1 and summarized in Table 2. Note that the calculated d-spacings of hd-Si are given to one digit less accuracy than the others to stay consistent with the lattice parameters given in the literature. The calculated values are the ambient condition values for the dc, bc8 and hd phases, the phases known to be (meta-)stable at ambient pressure and temperature. In the case of the metallic modifications of Si, for (β-Sn)-Si the pressure was 13 GPa [1] and for sh-Si 19.5 GPa.[5] Finally, the pressure in the case of r8-Si was 8.2 GPa.[7] Crystallographic databases were also consulted for confirmation and to obtain reflection conditions.[34–37]

The Si phases observed by electron and XRD are indexed after these known values. In this context, it is important to address the relative error of these two measurements. For electron diffraction, the d-spacings are determined from a photographic negative and the calibration of the electron microscope used. Since the calculated d-spacings are reciprocal to the measurement, the error associated with this calibration is also reciprocal, that is, it increases with increasing d-spacings. For the transmission electron microscopy (TEM) used in this study, this systematic error comes to ±0.1 Å for d-spacings between 4 and 6 Å. In contrast, synchrotron XRD yields a significantly higher accuracy and peak positions can be determined from peak fitting (provided no Rietveld refinement is performed). Where required, such peak fitting with Gaussian curves is

Table 1. The space groups and lattice parameters of the known crystal structures of the observed Si polymorphs from [33] for dc-Si, from [1] for (β-Sn)-Si, from [5] for sh-Si, from [2] for bc8-Si, from [4] for hd-Si and from [7] for r8-Si.

Phase	Space group	Lattice parameters
dc	$Fd\bar{3}m$	$a = 5.4307$ Å
(β-Sn)	$I4_1/amd$	$a = 4.686$ Å
		$c = 2.585$ Å
sh	P_6/mmm	$a = 2.527$ Å
		$c = 2.373$ Å
bc8	$Ia\bar{3}$	$a = 6.636$ Å
hd	$P6_3/mmc$	$a = 3.80$ Å
		$c = 6.28$ Å
r8	$R\bar{3}$	$a = 5.620$ Å
		$\gamma = 110.07^\circ$

Table 2. The reflection conditions of the observed Si polymorphs calculated after the literature values summarized in Table 1.

dc (Si-I)		β-Sn (Si-II)		sh (Si-V)		bc8 (Si-III)		hd (Si-IV)		r8 (Si-XII)	
hkl	d_{calc}	*hkl*	d_{calc}	*hkl*	d_{calc}	*hkl*	d_{calc}	*hkl*	d_{calc}	*hkl*	d_{calc}
111	3.125	200	2.343	001	2.373	110	4.695	100	3.29	100	4.501
220	1.920	101	2.263	100	2.188	200	3.318	002	3.14	$1\bar{1}1$	3.219
311	1.637	220	1.657	101	1.609	211	2.709	101	2.91	$2\bar{1}1$	2.659
		211	1.628	110	1.264	220[a]	2.346	102[a]	2.27	$20\bar{1}$	2.638
						321	1.774	110	1.90	$0\bar{1}1$	2.579
						400	1.659	103	1.77	200[a]	2.250
								200	1.65	$2\bar{1}\bar{2}$	2.050
								112	1.63	$1\bar{1}\bar{2}$	2.022
										$3\bar{2}1$	1.741
										$30\bar{2}$	1.735
										$3\bar{1}0$	1.718
										210	1.690
										$2\bar{2}\bar{2}$	1.610

[a] No significant experimental X-ray intensity has been observed for these *hkl* and hence they were not indexed in the XRDP.

conducted here using Origin,[38] which results in a relative error of ± 0.001 Å. Furthermore, it should also be noted that the use of electrons does not yield the same information on the relative peak intensities as X-rays do, thus preventing any Rietveld or similar refinements from being performed in the former case.

3. Experimental details

3.1. *Indentation studies*

A series of point loadings was performed on single-crystal Czochralski-grown Si(100), p-doped for a resistivity of 5–10 Ωcm using a so-called spherical diamond tip with $\sim 18\,\mu$m radius on a Ultra-Micro-Indentation-System 2000. The maximum load employed was 700 mN with an average unloading rate of ~ 1.2 mN/s. In the case of such a spherical tip, essentially consisting of a diamond ball, the contact area increases as the load is increased. Under the conditions used here, the presumed formation pressure of the metallic phase of 11.3 GPa is reached at a load of ~ 300 mN. Through further loading a transformed zone of $\sim 10\,\mu$m diameter and ~ 400 nm

depth containing the bc8/r8-Si mixture is always formed. Note that no fracturing is observed under these conditions. These transformed volumes were furnace annealed for 120 min at 200°C in a nitrogen atmosphere. For such indents, this has been shown to result in the formation of predominantly Si-XIII.[10]

Samples of such transformed volumes were prepared for TEM. Two different geometries of TEM sections were used. Cross-sectional TEM (XTEM) sections were prepared using an FEI xT Nova NanoLab 200 dual-beam focused ion beam (FIB) system employing the *ex situ* 'pluck-out' technique.[39] Since this technique allows for highly side-specific preparation of the TEM lamella, Raman spectra of the indents to be thinned were recorded prior to FIB processing using a Renishaw 2000 Raman imaging microscope with a HeNe laser (632.8 nm excitation line) focused to a spot of $\sim 1\,\mu$m radius. In this geometry, the electron beam is incident on the transformed volume *perpendicular* to the uniaxial pressure applied by the diamond tip. Plan-view samples were prepared from large arrays of indents placed in the center of 3 mm diameter Si discs. The discs were thinned to electron transparency using a Gatan dimple grinder 656 and wet etching with HNO3:HF:CH3COOH in a ratio of 5:1:1. In this geometry, the electron beam is incident on the transformed volume *parallel* to the uniaxial pressure applied.

The thinned TEM sections were imaged using a Philips CM 300 TEM operating at 300 kV. Selected area electron diffraction patterns (SAEDPs) of the transformed regions were taken on negatives. An aperture of $\sim$300 nm diameter was placed within the beam path to exclude the surrounding matrix. This results in SAEDPs solely from the transformed volume. Note that under these experimental conditions only a very small number of crystals are in a positive diffraction condition and thus recorded on the SAEDP. This is due to their random orientation and relatively low number in combination with the high sensitivity of electron diffraction to the exact orientation of a crystal.

3.2. *Formation of metastable polymorphs in DACs*

The thermal evolution of the metastable Si polymorphs was also investigated in a DAC. These studies were performed on single-crystal Si with the same properties as used for the point loading studies, but ground to powder using a new and clean mortar and pestle. Samples of this powder were placed into three different symmetrical DACs and one Boehler plate DAC.[40] All cells used diamond anvils with 300–400 μm culets. The gaskets had initial chambers of 150–160 μm diameter and 40–50 μm height. Rhenium was used as gasket material for the first three cells and stainless steel for cell 4. Three different pressure media were used, 4:1 methanol–ethanol for cell 1, neon for cells 2 and 4 (gas loading performed at GSECARS, Advanced Photon Source, Argonne National Laboratory) and argon for cell 3 (gas loading performed with a 0.3 GPa gas loader (Boehler), Geophysical Laboratory). Note that in these pressure regimes of interest for the metastable Si phases, all three pressure media are expected to be essentially hydrostatic under the conditions of this experiment.[41] A ruby ball ($\sim$ 10–20 μm) was added in all cases for pressure determination. Cells 1 and 2 were then equipped with High Pressure Collaborative Access Teams (HPCAT's) external resistive heaters [42] and a membrane for remote pressure control.

In situ powder XRD was performed at HPCAT, Advanced Photon Source, Argonne National Laboratory using the monochromatic X-rays of an insertion-device beamline (16 ID-B). A wavelength of 0.4072 Å (energy 30.45 keV) was used for cells 1, 3 and 4 and of 0.3738 Å (energy 33.17 keV) for cell 2. Diffraction patterns were collected with a MAR345 detector in the cases of cells 1 and 2 and with a Pilatus 1M-F detector in the cases of cells 3 and 4. The collected diffraction patterns were analyzed and reduced to integrated 2θ profiles using Fit-2D.[43,44] These X-ray diffraction patterns (XRDP) are displayed as a function of the scattering vector $Q = 4\pi \sin(\theta)/\lambda$.

For cells 1 and 2, pressure was increased online to above 15 GPa using the HPCAT membrane control system. This ensured full metallization of the dc-Si through complete conversion into sh-Si. Thereby, pressure was determined using the HPCAT online ruby system and the well-known pressure dependence of ruby,[45] while phase composition was confirmed from the XRDPs. After full metallization, pressure was decreased using the same system with the aim to form predominantly the bc8 and the r8 phase, respectively. In the methanol–ethanol-loaded cell 1, (β-Sn)-Si was present down to 9.5 GPa with further decompression resulting in complete transformation to r8-Si by 8.4 GPa. Continued unloading commenced the transition to bc8-Si at $\sim$7 GPa with the majority of r8-Si transformed at 4.6 GPa. When heating commenced, cell 1 had been unloaded to $\sim$3 GPa and the material consisted predominantly of bc8-Si. In the case of the Ne-loaded cell 2, solely (β-Sn)-Si was present down to 11.0 GPa. Upon further decrease to 10.4 GPa, r8-Si started to nucleate with predominantly r8-Si remaining at 8.5 GPa (a similar pressure as observed for cell 1). Upon heating, this cell had been settled at $\sim$10 GPa yielding predominantly r8-Si.[3]

Cell 3 was loaded to 18.5 GPa as determined via the ruby method using a Raman/ruby setup (Boehler, Geophysical Laboratory) equipped with a 473 nm laser. After metallization was confirmed optically (sh-Si is not Raman active [46]), the cell was decompressed slowly. Thereby the transition from metal to semiconductor (*i.e.* (β-Sn)-Si to r8-Si) was optically observed at 9.3 GPa, consistent with transition pressures in cells 1 and 2. Pressure was further decreased and stabilized at 3.6 GPa. The resulting phases were probed with Raman spectroscopy using the same Raman/ruby setup and laser. The Raman spectrum confirmed the presence of r8-Si and bc8-Si from the main r8-peak at $\sim$ 350 cm^{-1} and main bc8-peak at $\sim$ 430 cm^{-1}.[28] Although both peaks displayed equal intensity, this does not allow conclusions about the percentages of bc8-Si vs. r8-Si due to different scattering cross-sections of the semimetallic bc8-Si and semiconducting r8-Si. Nonetheless, it is clear that both polymorphs were present under these conditions.

3.3. *In situ heating in the DACs*

The isobars and isotherms explored are summarized in Figure 2(a), with the time dependence of the heating shown in Figure 2(b). Thereby, bc8-Si and r8-Si once formed in cells 1 and 2 were slowly heated using the external resistive heating to 200°C and 257°C, respectively. During the heating, pressure was monitored (and if necessary adjusted using the membrane) also with the HPCAT online ruby system employing additionally the ruby temperature corrections.[47] In the bc8-Si case (cell 1), the pressure drifted up to $\sim$4 GPa and then appeared to cycle by $\pm$0.3 GPa. In the r8-Si case (cell 2), the pressure similarly cycled between 9.8 and 11.0 GPa as long as the r8-Si remained present. After heating cell 1 for 2 h at 200°C, pressure was again increased to 19 GPa. During this pressure increase, the temperature drifted up to 214°C.

In the case of cell 3, the mixture of bc8-Si and r8-Si was laser heated with a ytterbium fiber laser ($\lambda = 1070$ nm, TEM00 mode, CW, IPG-Photonics) defocused to 0.5 W until melting of the Ar pressure medium occurred. This was confirmed visually using the laser speckle method.[48] At a pressure of 3.6 GPa, this corresponds to a temperature of 230°C.[49] Thus, the Si was heated, somewhat indirectly, by the surrounding liquid Ar to this same temperature. The Si was kept at 230°C for 6 min, then the laser was turned off to stop heating immediately. Thereafter, the phase composition was again investigated using Raman, but only hd-Si and/or nanocrystalline dc-Si was detected (both are almost indistinguishable by Raman [23]). To fully probe for the phase composition, cell 3 was hence investigated further using synchrotron X-ray radiation. However, the Ar used in this cell as pressure medium and temperature marker is frozen [49] at these conditions (3.6 GPa, 23°C). This results in strong Ar peaks overlapping with the Si peaks of interest. Therefore, the same phase composition as present prior to heating was also created in an

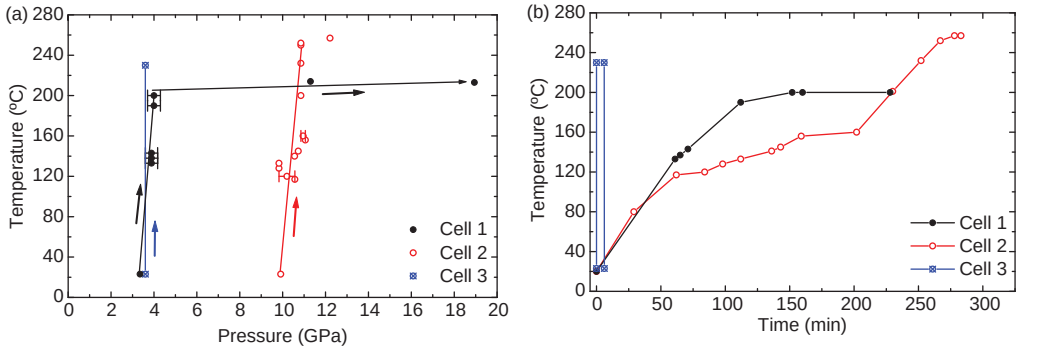

Figure 2. (Color online) Heating conditions for the three heated cells depicted as temperature vs. (a) pressure and (b) time.

additional cell (cell 4) but with Ne as pressure medium (which does not freeze until higher pressures). To ensure the same phase composition, cell 4 was also manually compressed to 19.8 GPa resulting in pure sh-Si and then slowly decompressed to 3.5 GPa. In this case, pressure was monitored using the HCPAT offline Raman kit and phase composition was confirmed using XRDPs. Thus, the Si polymorphs present in cell 4 provide a reference for the heated polymorphs in cell 3.

4. Results

4.1. *Annealing of the bc8/r8 mixture made by point loading*

A typical Raman spectrum of an annealed (200°C) bc8/r8-Si mixture made by point loading is shown in Figure 3(a). Some signature of bc8/r8-Si [28] remains as indicated in the graph. The majority of the initial bc8/r8-Si mixture, however, has transformed to a new phase as indicated by the Raman bands at $\sim$202, $\sim$333, $\sim$478 and possibly $\sim$500 cm^{-1}. The first three bands represent the unidentified phase Si-XIII,[9,10] but the band at $\sim$ 500 cm^{-1} may be attributed to either hd-Si or Si-XIII.[9,10] This indent was prepared for XTEM and the resulting SAEDP is shown in Figure 3(b). In addition to polycrystalline rings representing dc-Si, a row of diffraction spots (indicated by yellow arrows) with an interatomic d-spacing of 5.6 $\pm$ 0.1 Å is observed. This does not correspond to any known Si polymorph, and it is thus clear that Si-XIII is also observed by SAEDP. An example of an SAEDP from an indent prepared in plan-view geometry is shown in Figure 3(c). As in the XTEM case, rows of diffraction spots (indicated by green and red arrows) are seen. Their interatomic spacing is 4.8 $\pm$ 0.1 and 4.4 $\pm$ 0.1 Å, which also does not match any known Si phase. The angles of 63° and 54° between these planes are also indicated. This latter SAEDP is captured from one single crystal, consistent with dark-field imaging performed in this case (not shown). Thereby, only one crystal was illuminated when either the 4.8/4.4 Å spots was used to form an image. Note that several XTEM and plan-view indents were investigated and these same d-spacings were repeatably observed. Some directional preference seems to exist, however, since the 5.6 $\pm$ 0.1 Å spacing was never observed in plan-view samples.

Although Si-XIII is kinetically stable once formed in residual indent impressions ($\sim$1 week at 200°C [10]), it is not kinetically stable in TEM sections. Firstly, it has been shown that only TEM sections of sufficient thicknesses contain Si-XIII.[9] Moreover, when investigated with the electron beam, Si-XIII anneals to dc-Si within minutes. Finally, even if not exposed to the electron beam, Si-XIII in thinned sections remains kinetically stable only for $\sim$1 week at room temperature before it is fully transformed to dc-Si. In combination with the small crystal size of

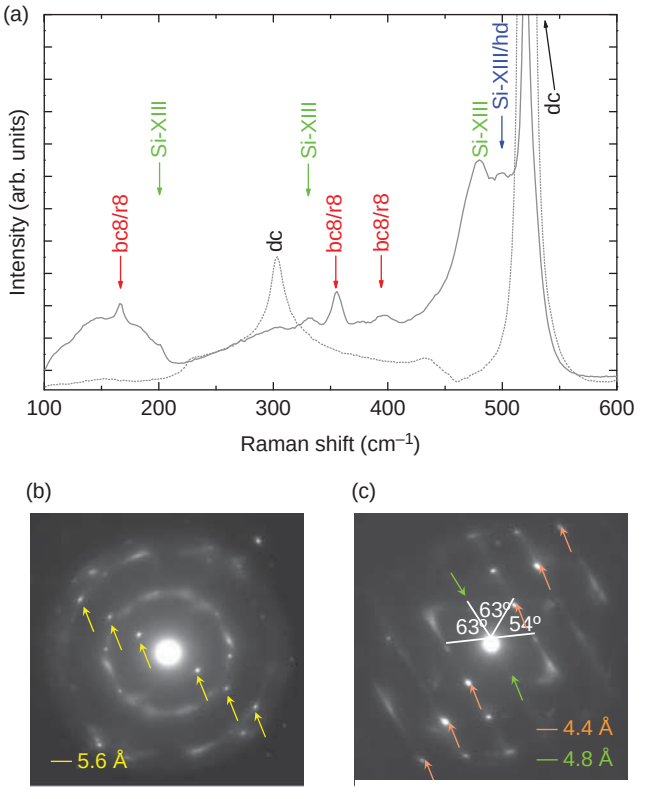

Figure 3. (Color online) (a) Raman spectrum of annealed bc8/r8-Si made by point loading (solid line) with the pristine dc-Si as background (dotted line). The peaks associated with the known different metastable Si polymorphs are indicated. SAEDPs taken from (b) this annealed phase transformed area in a cross-sectional geometry and (c) a different area in plan-view geometry. The rows of diffraction spots that correspond to *d*-spacings not matching any known Si polymorph are indicated by arrows. In (c) several rows corresponding to these *d*-spacings are seen and the angle measured between these lattice planes are also indicated.

$\sim$10–30 nm,[28] this prohibits any further investigation by TEM. Note, however, that the formation of pure dc-Si under these conditions indicates that Si-XIII is indeed a pure Si polymorph itself.

4.2. *Annealing in a DAC*

XRD data from cell 1 containing predominantly bc8-Si are shown in Figure 4(a). This material was thermally annealed at the constant pressure of $\sim$4 GPa to 200°C. At 133°C two new peaks appear in the integrated XRDP as indicated by arrows. The *d*-spacings of the two unknown peaks were determined from peak fitting to 2.394 ± 0.001 and 2.113 ± 0.001 Å. Although the transient nature of these peaks suggests they are not due to contamination, investigation of the 2D XRDP taken at 133°C shown in Figure 4(b) confirmed that they are Si peaks. The bc8-Si rings (in red) are indexed after Table 2. A distinct shoulder on the (211) ring is attributed to the presence of small volumes of r8-Si. Interestingly, the unknown peaks clearly arise from powder diffraction and the rings are indicated (in green) in the figure. This strongly suggests that these peaks do indeed correspond to another Si polymorph. However, upon further heating to $\sim$ 140°C they disappeared, and hd-Si was observed to form. Upon further heating almost all material had transformed to hd-Si at $\sim$ 200°C. The cell was kept at this temperature for another 120 min

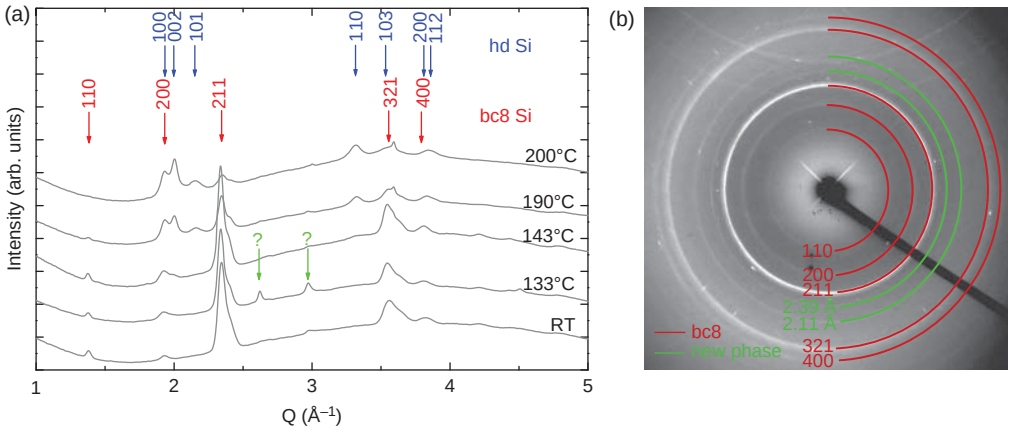

Figure 4. (Color online) (a) Integrated XRDP of the evolution of bc8-Si under thermal annealing at 3 GPa in cell 1. The room temperature bc8-Si and the final hd polymorph at 200°C are indexed. For increasing annealing temperatures, the spectra are offset for clarity. Between 130°C and 140°C unidentified peaks appear as indicated. (b) A full 2D diffraction pattern of the spectrum at 133°C with the powder rings responsible for these two unknown peaks indicated by their *d*-spacing.

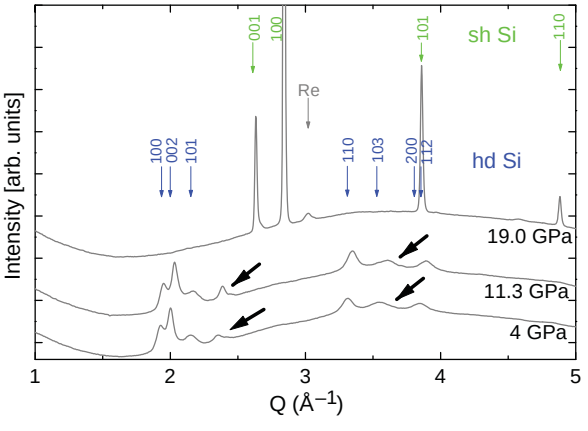

Figure 5. (Color online) Integrated XRDP of hd-Si pressurized at ∼ 215°C. The hd-Si and sh-Si are indexed and the r8-Si component is indicated by bold arrows.

(Figure 5) and no further change was observed. Note that the r8-Si $(20\bar{1})$ and bc8-Si (211) peaks overlap and thus the remaining material that is not transformed to hd-Si is attributed to r8-Si.

To investigate the transition pathway of hd-Si on compression, cell 1 was re-pressurized to 19 GPa at a constant temperature of ∼ 200°C. The resulting XRDPs are shown in Figure 5. The XRDP at 4 GPa represents the same material as shown in Figure 4(a) at 200°C, but after annealing continuously for 120 min at this temperature. Clearly, this annealing made no difference to the hd-Si nor the r8-Si component. Upon increasing pressure to 11.3 GPa, no metallization had occurred yet and the hd-Si and r8-Si remained essentially unchanged. Upon further compression to ∼ 19 GPa, formation of a metallic phase occurred. In this particular case, the formation of nucleation seeds of the metallic phase could be clearly observed optically within the semiconducting matrix. These seeds grew until the entire Si material was metallized after ∼ 10 mins. The XRDP taken after this full metallization confirms the sole presence of the metallic sh-Si.

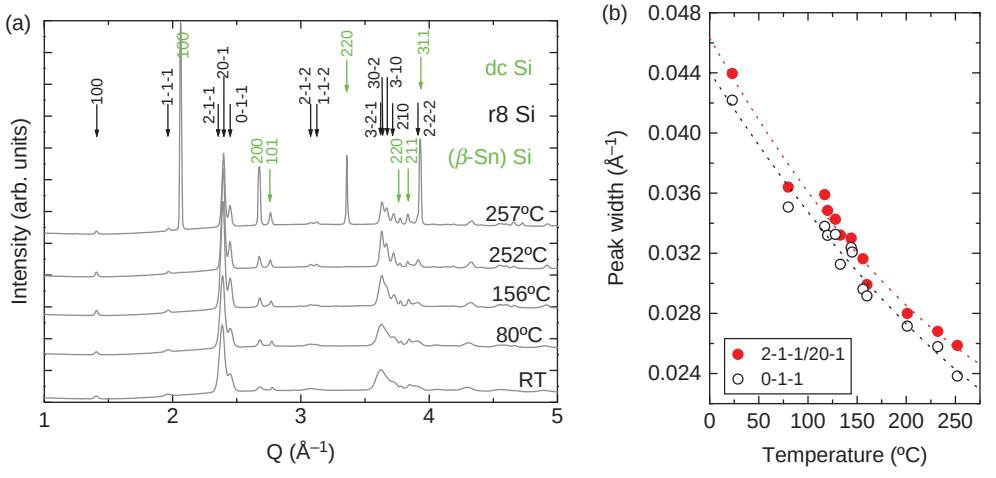

Figure 6. (Color online) (a) Integrated XRDP of the evolution of r8-Si under thermal annealing at ∼10 GPa in cell 2. The room temperature r8-Si and the final dc-Si at 257°C are indexed together with the presence of (β-Sn)-Si. For increasing annealing temperatures, the spectra are of-set for clarity. (b) Development of the peak width with temperature of the convoluted $2\bar{1}1/20\bar{1}$ and the $01\bar{1}$ r8 peaks. The widths are extracted from peak fitting with Gaussians and are shown together with polynomial fits to the data.

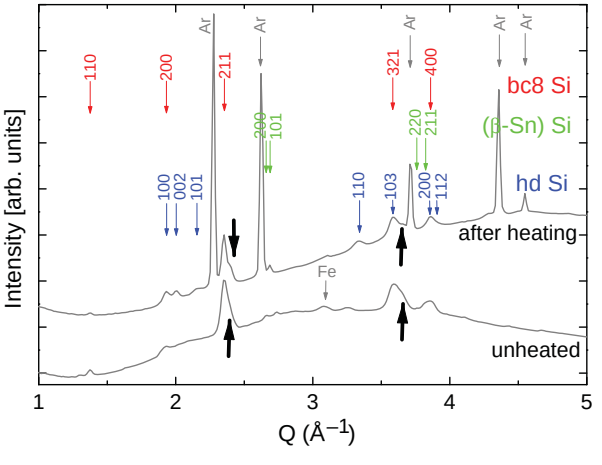

Figure 7. (Color online) Integrated XRD spectra of bc8- and r8-Si laser heated at 230°C for 6 min at 3.6 GPa (after heating). For comparison, unheated material at 3.5 GPa is also shown (unheated). The hd, bc8 and (β-Sn) polymorphs are indexed and the r8-Si component is indicated by bold arrows.

Cell 2, which contained r8-Si with some (β-Sn)-Si, was heated to 257°C at the constant pressure of ∼10 GPa and the resulting XRDPs are shown in Figure 6(a). Up to 252°C no phase transitions are observed and instead the r8-Si peaks sharpen. This sharpening is shown in Figure 6(b) for the example of the first dominant set of r8-Si peaks. The peaks were fitted with Gaussians using Origin.[38] Upon further heating to above 252°C a sudden transition to dc-Si occurred. This was accompanied by a sudden pressure increase of ∼1 GPa attributed to the ∼9% volume increase from r8-Si to dc-Si. This also resulted in a small increase in volume of (β-Sn)-Si. Since the pressure in the DAC was at 12.2 GPa, the dc-Si peaks are shifted to higher Q-values (and thus smaller d-spacings) compared to the ambient pressure values in Table 2. Furthermore, the dc-Si rings appeared very spotty in the 2D XRDP (not shown) suggesting that

large crystals nucleated very suddenly from r8-Si at this temperature. No evidence of any other intermediate phases was detected.

As shown in Figure 2(b), the external resistive heating in the above cases always required a time of several hours that was accompanied by a continuous up-drift in pressure. It may be expected that this would influence nucleation kinetics. Therefore, in a final heating experiment laser heating was performed at 3.6 GPa. Such laser-heating results in near instantaneous heating of the Si material at truly constant pressure and can thus provide different insights compared to the *ex situ* heating. Therefore, the metastable Si polymorphs heated to 230°C for 6 min at 3.6 GPa are shown together with a reference XRDP of unheated material at 3.5 GPa in Figure 7. Both XRDPs indicate the presence of a remanent of (β-Sn)-Si together with metastable phases. In the unheated case, predominantly bc8-Si appears present with a component of r8-Si as indicated by bold arrows. Laser heating appears to transform this bc8-Si into hd-Si within 6 min of heating, but the r8-Si remains. Note that this r8-Si component was not observed by Raman spectroscopy.

5. Discussion

5.1. *Influence of hydrostaticity on the formation of the bc8 and r8 polymorphs*

Before considering the thermal evolution of the bc8 and r8 phases made in a DAC, let us compare first our observed transition pressures on loading and unloading at room temperature to those reported in the literature. Two examples employing different pressure media (methanol–ethanol and neon) will be discussed.

For unloading from metallic Si, Piltz et al.[7] report the formation of r8-Si at $\sim$9 GPa (when using methanol–ethanol). This appears consistent with our observation of a sharp transition of (β-Sn)-Si to r8-Si between 9.5 and 8.4 GPa in the methanol–ethanol-loaded cell 1. In contrast, the formation of r8-Si in the Ne-loaded cell 2 commences at the somewhat higher pressure of $\sim$10.4 GPa. (Almost) full transformation to r8-Si, however, is not achieved until 8.4 GPa, similar to the methanol–ethanol case. The formation of r8-Si at this relatively high pressure may be attributed to the low shear resulting from Ne as pressure medium compared to methanol–ethanol.[41] The previous study also reported 2.8 GPa as the pressure for the reversible transition between bc8-Si and r8-Si.[7] This pressure appears considerably higher in our case, where bc8-Si commences to form at 6.3 GPa. Since the same experimental conditions as in [7] are used, the reason for this higher pressure in our study is unclear.

The implications of different degrees of hydrostaticity on the phases in the metallic regime may, however, be more interesting. Although both pressure media are similarly hydrostatic in the regime used for thermal annealing ($\leq$11 GPa), they are not similarly hydrostatic in the metallic (β-Sn)-Si regime ($\geq$11 GPa).[41] While the Ne (albeit frozen) remains quasi-hydrostatic, the frozen methanol–ethanol induces significant strain above $\sim$11 GPa.[41] This results in structural differences in the (β-Sn)-Si formed[4] which may also influence the structure of the r8-Si and bc8-Si formed on pressure release. Thus, although we note that both pressure media are hydrostatic in the metastable regime, the resultant phases may still differ as their respective (β-Sn) parent phases may not be identical in nature.

5.2. *Metallization of hexagonal diamond Si*

Our study shows that upon compression to 11.3 GPa at $\sim$200°C hd-Si remains kinetically stable. Only upon further compression does this polymorph metallize, in our case into sh-Si at 19 GPa. No reports exist in the literature on the metallization of hd-Si upon compression, and it remains

unconfirmed whether it transforms into (β-Sn)-Si or directly into sh-Si. It is, however, interesting to compare its metallization to that of r8-Si and dc-Si.

The data presented in this current study show that at elevated temperatures r8-Si transforms into (β-Sn)-Si below 11 GPa. Thus, hd-Si (that is unchanged at 11.3 GPa at $\sim$ 200°C) exhibits a larger kinetic stability against metallization than r8-Si. This may be attributed to the fact that hd-Si possesses the same tetrahedral bonding as dc-Si (*i.e.* a lonsdaleite or wurtzite-type structure with consequently the same perfect tetrahedral bond angle, same ideal Si-Si bond length and same mass density [2]). This is different for r8-Si with its strained bond angle and bond length and increased mass density.[7]

No data on the metallization of dc-Si at elevated temperature were obtained in this current study. However, the onset of the formation of (β-Sn)-Si from dc-Si does not vary with room temperature (only the coexistence regime of dc-Si and (β-Sn)-Si does).[50] Thus, comparison of the metallization of our hd-Si at $\sim$200°C to that of dc-Si at room temperature is warranted if the same pressure medium is used. No comparison with the metallization of dc-Si from the same experimental run (cell 1) is possible, since no data ware taken for this case (attaching the membrane increased pressure and resulted in full metallization). The literature, however, reports the pressure of the transformation of dc-Si into (β-Sn)-Si as ranging from 10.3 [6] to 11.7 GPa [25] when methanol–ethanol was used. It thus appears that hd-Si does not metallize at lower pressures than dc-Si.

5.3. *Thermal evolution of the bc8 and r8 polymorphs in a DAC*

Previous experiments at ambient pressure reported the formation of hd-Si from bc8-Si at 200°C.[2,4] In the present study, this same transition was also observed at 4 GPa but commencing at the lower temperature of 140°C. This indicates that the transition temperature for the bc8-Si to hd-Si transition decreases with increasing pressure. This is consistent with a literature report [2] of a lower transition temperature at higher pressures for bc8-Si. Furthermore, the transition between bc8-Si and hd-Si occurs very fast as shown by our laser-heating experiment. Both these observations suggest a well-defined, distinct boundary for the irreversible transition from bc8-Si to hd-Si.

Intriguingly, prior to the formation of the hd structure, an additional intermediate phase appears to form between 130°C and 140°C. This phase was not observed upon laser heating for 6 min. Since this phase may be related to the Si-XIII structure formed upon bc8/r8-Si made by point loading, it will be discussed in more detail in Section 5.4.

It is noted that no annealing studies of r8-Si have been performed previously. Our results show that r8-Si is more stable at elevated temperatures than bc8-Si and (at around 10 GPa) it transforms directly to dc-Si. Furthermore, upon annealing a significant sharpening of the r8-Si peaks was observed. This may suggest a growth in crystal size. (Relaxation of stress, which could also explain this observation, appears less likely since the r8-Si formed under quasi-hydrostatic conditions.) Such behavior was not observed for bc8-Si. Moreover, the transition to dc-Si is surprisingly abrupt (within 5°C only) and not much dc-Si was observed prior to this transition. Therefore, this may suggest a strong kinetic energy barrier between r8-Si and dc-Si.

5.4. *Formation of the Si-XIII polymorph*

The Si-XIII phase forms as an intermediate phase on the path to dc-Si if bc8/r8-Si is made by point loading. In this current study, *d*-spacings that cannot be matched to any other known polymorph of Si were observed for Si-XIII made by point loading. A recent theoretical study

using particle swarm optimization methods presented a tetragonal structure as a solution of Si-XIII.[51] This proposed structure, however, does not exhibit all the known Si-XIII Raman bands and, furthermore, does not correspond to the electron diffraction data presented here. Thus, the Raman spectroscopy and electron diffraction conducted in the current study both confirm that an unidentified phase, Si-XIII, exists, but its structure remains elusive.

Nevertheless, it is interesting to consider the insights obtained on the formation of Si-XIII from bc8/r8-Si made via point loading in more depth. Firstly, the bc8/r8-Si made by point loading acts like a single phase since the entire bc8/r8-Si phase mixture transforms fully into another phase, that is, Si-XIII, upon thermal heating. In contrast, in a DAC, the bc8-Si component always transformed into hd-Si and the r8-Si component into dc-Si. This may suggest that bc8/r8-Si is one single hybrid phase that can only be formed by point loading instead of a true mixture of bc8-Si and r8-Si as formed in a DAC.

Furthermore, this current study shows the presence of considerable preferential orientation in the Si-XIII formed. This can be expected to arise from the nature of the bc8/r8-Si that is created by point loading. This is also clearly different to our DAC cases where non-preferential powder was used.

Additionally, the geometry of the transformed zone created by point loading results in a direction of non-confinement, that is, the surface. This allows for the formation of a phase of lower density than bc8/r8-Si or dc-Si. In contrast, the tendency of DACs to increase pressure upon heating inhibits such a volume increase necessary for the formation of a lower density phase. If Si-XIII is such a lower density phase, this could prevent its formation in DACs, but favor other intermediate phases, namely hd-Si.

Finally, the fact that Si-XIII is not readily observed upon annealing of bc8-Si made in a DAC,[32] but only upon annealing of bc8/r8-Si made via point loading,[9,10,32] has previously been attributed to differences in residual stresses.[32] Transformed volumes made by point loading can contain a certain degree of residual stresses. In the present case, this has been estimated to be ~ 1 GPa.[10] It was thus speculated that these high residual stresses give rise to the formation of Si-XIII on annealing. Our observations of Si-XIII instability following TEM sample preparation would seem consistent with this scenario. Namely, Si-XIII confined within a Si matrix appears metastable 'indefinitely', but once the material is thinned (which results in relieving of residual stresses), the lifetime is decreased to less than 1 week. It is therefore quite possible that Si-XIII can only form at pressures above ~ 1 GPa from bc8/r8-Si.

In the case of *in situ* DAC annealing, the appearance of the two unknown peaks at 133°C between bc8-Si at lower temperatures and hd-Si at higher temperatures (Figure 4) may be related to Si-XIII. The XRD peaks at 2.394 ± 0.001 and 2.113 ± 0.001 Å could match the 4.8 ± 0.1 and 4.4 ± 0.1 Å measured by electron diffraction as second-order (Si-XIII) planes (considering the large error in SAEDP analysis and higher pressure in the DAC case).[5] The XRD data are, however, not sufficient to speculate further on this.

Thus, many open questions remain about this intriguing polymorph. Foremost, its exact structure still remains unresolved. Additionally, it is unclear why it can be easily formed from the bc8/r8-Si made by point loading, and not readily from bc8-Si or r8-Si made in a DAC. It is therefore at the current stage not possible to determine the metastability regime of Si-XIII with any certainty.

5.5. *Stability regimes of the metastable phases*

The pressure and temperature dependence of the formation of the other metastable Si phases can be represented by their (meta-)stability regimes. Although such a plot may resemble a phase diagram, it should not be construed as such, since the only truly stable phases in the regimes

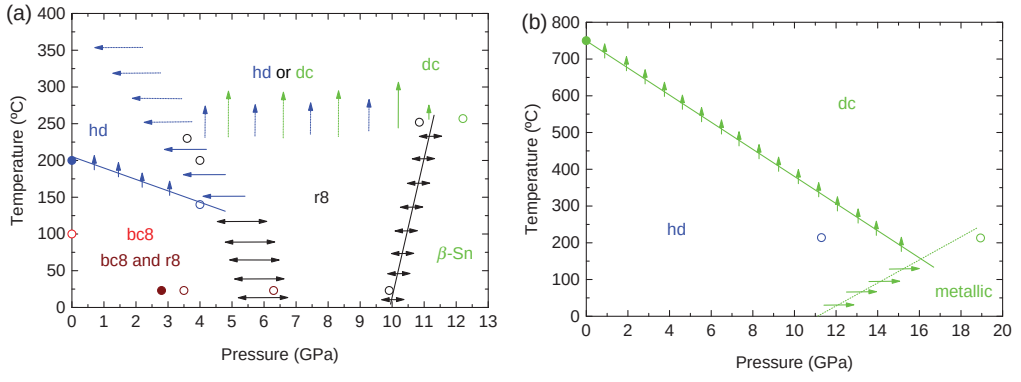

Figure 8. (Color online) Diagram of the transitions pathways in the metastability regimes of the (a) bc8 and r8 polymorphs and (c) the hd polymorph. The irreversibility and reversibility of these transitions are indicated by single-sided and double-sided arrows, respectively. Data points from our observations and literature are depicted with open and closed circles, respectively. Solid lines indicate now identified dP/dT slopes in this diagram, whereas dashed lines are suggestions for less well-identified dP/dT slopes. The absence of lines indicates transition boundaries where no dP/dT slopes can be defined. For further details refer to text.

considered here are dc-Si, (β-Sn)-Si and sh-Si. Instead, such a diagram represents the transition pathways that can lead to the different polymorphs. Our investigation of the metastable phases of Si yields a number of important insights for such a diagram. The suggested transition pathways and (meta-)stability regimes are summarized for bc8-Si and r8-Si in Figure 8(a) and for hd-Si in Figure 8(b). Based on our new data and the literature, a number of previously unknown slopes of 'pathway boundaries' can now be determined.[6]

Let us consider the metastability regime of the bc8 polymorph first. Firstly, the formation of hd-Si from bc8-Si at $\sim$140°C and 4 GPa (when the same transition occurs at $\sim$200°C at ambient pressures [2,4]) indicates a negative dP/dT slope for the irreversible bc8-Si to hd-Si transition. Matters are less clear for the reversible bc8-r8 transition. Although r8-Si is solely present above $\sim$6 GPa, it remains unknown if decompression can yield pure bc8-Si and in our study a remanent of r8-Si was always observed. This is consistent with the literature where the presence of r8-Si has been noted upon full decompression using XRDP [7] and Raman (albeit not identified as r8-Si at the time).[52] Indeed, Piltz et al.report that heating to 100°C did reduce the r8-component.[7] Although moderate heating directly below the bc8-hd transition boundary may conceivably yield pure bc8-Si, this has not been observed experimentally. Furthermore, this coexistence clearly prevents a definition of the dP/dT slope for the reversible bc8-r8 transition.

The metastability regime of r8-Si is discussed next. Our data clearly demonstrate that r8-Si can exist as the sole metastable phase in a relatively large regime. Indeed, an increased kinetic stability over bc8-Si with respect to temperature has been demonstrated at pressures as low as 3.6 GPa and as high as 10 GPa. Furthermore, knowledge about some of the dP/dT slopes has been gained. For r8-Si four slopes/transition pathways exist, metallization under compression, transitions upon heating and transitions upon decompression above and within the bc8-Si metastability field. Firstly, our observation of predominantly r8-Si with a small component of (β-Sn)-Si below 10 GPa at ambient temperature and the same at 11 GPa at $\sim$ 250°C indicates a positive dP/dT slope for the reversible r8-Si to (β-Sn)-Si transition. Secondly, the observed nucleation of dc-Si from r8-Si at 10 GPa and $\sim$255°C without any hint of hd-Si may suggest that r8-Si always transforms to dc-Si upon heating. Our data, however, cannot fully exclude that a regime at lower pressure may exist where r8-Si can also transform into hd-Si upon heating. Equally, it is not entirely clear if r8-Si transforms into hd-Si or dc-Si upon decompression above the bc8-Si metastability regime (*i.e.* above 140°C). Hence, these dP/dT slopes remain undetermined. Nonetheless, it is clear that, unsurprisingly, compression of hd-Si does not result in

transformation to r8-Si. Therefore, any r8-hd transition is, identically to the bc8-hd transition, irreversible.

Finally, our compression experiment of hd-Si at $\sim$200°C also yields insight into the metastability regime of this polymorph. Based on the nucleation of metallic Si (sh-Si) at 19 GPa together with the previously reported temperature of the hd-Si to dc-Si transition of $\sim$ 750°C at ambient pressure,[31] our data clearly indicate a negative dP/dT slope for the irreversible hd-Si to dc-Si transition. The dP/dT slope of the hd-Si to (β-Sn)-Si transition is less clear. It appears unlikely, however, that hd-Si transforms to (β-Sn)-Si at a significantly lower pressure than dc-Si. Hence no temperature dependence (*i.e.* akin to dc-Si) or a negative dP/dT slope can be assumed for this irreversible transition.

Many open questions remain. For example, in our experiments it was difficult to control decompression at elevated temperatures, which is necessary to investigate the r8-Si stability further. This may be overcome through the use of the newly developed dynamic compression setup utilizing two membranes.[53] Similarly, the exploration of the hd–dc transition boundary requires heating that is high for resistive heating and too low for laser heating. Intriguingly, it may be possible to explore these transition pathways and dP/dT slopes on a related system, that is, germanium, where the same pathways can be observed, but at significantly lower temperature.[53] Study of this analogous system could thus answer many open questions also about Si.

5.6. *Stability of the r8 polymorph*

The observations made here are important for potential applications of the r8 phase. As detailed above, r8-Si may possess highly desirable properties for photovoltaic [14] and other applications [12] and its stability is therefore relevant. Therefore, implications from the metastability regime determined from our DAC studies are considered first, before the potential for exploitations of this phase is discussed.

In our DAC study, no evidence for a thermal instability of r8-Si prior to its transition to dc-Si can be detected. Namely, upon heating the r8 crystals do not commence to decompose, but instead grow in size. Furthermore, the constant presence of similar volumes of r8-Si and (β-Sn)-Si upon heating is reminiscent of the phase boundary between two stable phases. Finally, the abrupt transition between r8-Si and dc-Si indicates a very strong kinetic barrier between these phases. All these observations suggest that in its metastability regime, r8-Si acts more like a truly stable structure rather than a metastable one.

The transition pathways depicted in Figure 8 for DAC (de)compression appear to suggest, however, that pure r8-Si cannot be stabilized at pressures below $\sim$3 GPa in a DAC upon decompression at room temperature. From the metastability regime shown in Figure 8(a), variation of temperature suggests further possibilities. Firstly, r8-Si could be maintained at lower pressures provided temperature is lowered sufficiently.[7] Similarly, r8-Si could exist at lower pressures, if temperature during decompression from the r8-Si metastability regime is increased to above the bc8-Si metastability regime (*i.e.* above 150°C).

For applications, it would be advantageous, however, to lower these pressures to true ambient. Indeed, point loading experiments have reported predominantly r8-Si metastable at 'ambient' pressure [12] albeit confined in an indent volume with a residual stress of $\sim$1 GPa. Such volumes of bc8/r8-Si can be exploited, for example, for maskless nanoscale patterning [30] or writing of electrically conductive and insulating zones.[29] As stated previously, the exact nature of this mixture of bc8/r8-Si is unknown, but it would be clearly beneficial to increase the r8-Si content. This could conceivably be achieved through doping. For example, doping the original parent dc-Si structure with germanium is promising since for Ge the bc8-r8 transition occurs as low as

0.5 GPa.[53] Indeed, transformed volumes of Ge made by point loading consist almost entirely of r8-Ge.[56] It thus appears clearly possible that sufficient r8-Si may be stabilized at pressures low enough to be exploited in a technological manner.

6. Conclusion

This current study presents interesting insights into the regime of metastable Si phases. Our findings allow for the construction of diagrams of the metastability regimes of bc8-Si, r8-Si and also hd-Si. These suggest negative dP/dT slopes for most irreversible transitions (bc8-Si to hd-Si, hd-Si to dc-Si, possibly also hd-Si to metallic Si, r8-Si to hd-Si and r8-Si to hd-Si or dc-Si) and a positive dP/dT for the reversible r8-Si to (β-Sn)-Si transition. Moreover, a relatively large regime in which pure r8-Si is stable can be identified. This latter finding may also become relevant for any potential application of this polymorph. Furthermore, we confirm that if a bc8/r8-Si mixture is made by point loading, thermal annealing results in a new phase, Si-XIII. This phase exhibits *d*-spacings that cannot be attributed to any known or postulated phase and its structure thus remains undetermined. This situation is different if the bc8 and r8 polymorphs are annealed *in situ* in a DAC. In the case of bc8-Si, hd-Si is formed at lower temperatures than observed at ambient pressure. A hint of an additional intermediate phase is observed which appears to form prior to the transition to hd-Si. Compression of this hd-Si at elevated temperature reveals an onset of metallization pressure for hd-Si at least as high as that of dc-Si. Furthermore, it was found that r8-Si transforms directly to dc-Si in a DAC at a critical temperature of 255°C. Finally, the thermal stability of bc8/r8-Si made by point loading ($\sim$200°C at ambient pressure) is encouraging for exploitation as it has previously been found to exhibit interesting semiconducting properties.

Acknowledgments

We would like to acknowledge and thank Reinhard Boehler and Amol Karandikar (both Geophysical Laboratory, Carnegie Institution, USA) for their assistance in conceiving and conducting the laser-heating experiment. Additionally, we would also like to thank Brad D. Malone (Harvard University, USA) and Marvin L. Cohen (University of California, Berkeley, USA) for many helpful and stimulating discussions. The XRD was performed at HPCAT (Sector 16), and the gas loading at GSECARS (Sector 13), both Advanced Photon Source (APS), Argonne National Laboratory. We also acknowledge the facilities and the technical assistance of the Australian Microscopy & Microanalysis Research Facility at the Electron Microscopy Unit, University of New South Wales, Australia, and the Center for Advanced Microscopy, Australian National University, Australia.

Disclosure statement

No potential conflict of interest was reported by the authors.

Funding

This work was supported by funding from the Australian Research Council (ARC). JEB is supported by an ARC Future Fellowship. Work by MG was fully supported by EFree, an Energy Frontier Research Center funded by the U.S. Department of Energy, Office of Science, Basic Energy Sciences under Award No. DE-SC0001057. BH acknowledges current funding through an Alvin M. Weinberg Fellowship (ORNL) and the Spallation Neutron Source (ORNL), sponsored by the U.S. Department of Energy, Office of Basic Energy Sciences. HPCAT operations are supported by DOE-NNSA under Award No. DE-NA0001974 and DOE-BES under Award No. DE-FG02-99ER45775, with partial instrumentation funding by NSF. Use of the COMPRES-GSECARS gas loading system was supported by COMPRES under NSF Cooperative Agreement EAR 11-57758 and by GSECARS through NSF grant EAR-1128799 and DOE grant DE-FG02-94ER14466. APS is supported by DOE-BES, under Contract No. DE-AC02-06CH11357.

Notes

1. Note that traditionally these different Si polymorphs are often denoted by Roman numbers (Si-I, Si-II, Si-III, etc.). In this work, we used the alternative denomination of a phase by its structural description (dc-Si, (β-Sn)-Si, bc8-Si, etc.) instead for two reasons. Firstly, none of the predicted phases are included within this numbering system, and secondly, denomination by structural description simplifies the comparison with other elements that possess structurally equivalent polymorphs such as germanium.
2. Note that the exact nature of the polymorph(s) obtained via such point loading is ambiguous. Namely, the exact ratio of the phases in the transformed volume is not known and it may even be possible that a hybrid mixed bc8/r8 phase is formed. The phases(s) made by point loading will therefore be referred to as bc8/r8-Si henceforth.
3. Note that in both cases, pressure was cycled by a few GPa to achieve the desired phase composition and stabilize the cells.
4. The (200) (β-Sn) peak is sharper in the Ne cell 2 compared to the methanol–ethanol cell 1, presumably due to strain in the latter case. Additionally, comparison of two cases where the (200) (β-Sn) peaks are at the same Q reveals a (101) peak shifted to a slightly lower Q for the Ne cell suggesting a slightly larger c/a ratio in this case.
5. Note that all peaks from allowed reflections have full intensity in electron diffraction, making them readily observable but that the same reflections can have low intensity in XRD. Hence the absence of peaks at 5.6 ± 0.1 Å, 4.8 ± 0.1 Å and 4.4 ± 0.1 Å in the XRD data could be attributed to these differences.
6. Note that Figure 8(a) does not consider bc8/r8-Si made from point loading that leads to Si-XIII.
7. Note that such cooling has to take place once r8-Si has already formed from (β-Sn)-Si because decompression from the metallic regime at low temperatures to pressures below 2 GPa does not result in r8-Si, but in (β-Sn)-Si followed by amorphization upon heating to ambient temperature.[54,55]

References

[1] Jamieson JC. Crystal structures at high pressures of metallic modifications of silicon and germanium. Science. 1963;139:762–764.
[2] Wentorf RH Jr, Kasper JS. Two new forms of silicon. Science. 1963;139(3552):338–339.
[3] Kasper JS, Richards SM. The crystal structures of new forms of silicon and germanium. Acta Crystallogr. 1964;17:752–755.
[4] Kasper JS, Wentorf RH Jr. Hexagonal (wurtzite) silicon. Science. 1977;197(4303):599.
[5] Olijnyk H, Sikka SK, Holzapfel WB. Structural phase transitions in Si and Ge under pressures up to 50 GPa. Phys Lett. 1984;103A(3):137–140.
[6] McMahon MI, Nelmes RJ. New high-pressure phase of Si. Phys Rev B. 1993;47(13):8337–8340.
[7] Piltz RO, Maclean JR, Clark SJ, Ackland GJ, Hatton PD, Crain J. Structure and properties of silicon XII. A complex tetrahedrally bonded phase. Phys Rev B. 1995;52(6):4072–4085.
[8] Hanfland M, Schwarz U, Syassen K, Takemura K. Crystal structure of the high-pressure phase silicon VI. Phys Rev Lett. 1999;82:1197–1200.
[9] Ge D, Domnich V, Gogotsi Y. Thermal stability of metastable silicon phases produced by nanoindentation. J Appl Phys. 2004;95(5):2725–2731.
[10] Ruffell S, Haberl B, Koenig S, Bradby JE, Williams JS. Annealing of nanoindentation-induced high pressure crystalline phases created in crystalline and amorphous silicon. J Appl Phys. 2009;105:093513 09351 093513–1–093513–8.
[11] Besson JM, Mokhtari EH, Gonzalez J, Weill G. Electrical properties of semimetallic silicon III and semiconductive silicon IV at ambient pressure. Phys Rev Lett. 1987;59(4):473–476.
[12] Ruffell S, Sears K, Knights AP, Bradby JE, Williams JS. Experimental evidence for semiconducting behavior of Si-XII. Phys Rev B. 2011;83:075316-1–075316-6.
[13] Wippermann S, Vörös M, Rocca D, Gali A, Zimanyi G, Galli G. High-pressure core structures of Si nanoparticles for solar energy conversion. Phys Rev Lett. 2013;110:046804-1–046804-6.
[14] Malone BD, Sau JD, Cohen ML. Ab initio study of the optical properties of Si-XII. Phys Rev B. 2008;78:161202-1–161202-4.
[15] Malone BD, Sau JD, Cohen ML. Ab initio survey of the electronic structure of tetrahedrally bonded phases of silicon. Phys Rev B. 2008;78:035210-1–035210-7.
[16] Malone BD, Cohen ML. Prediction of a metastable phase of silicon in the Ibam structure. Phys Rev B. 2012;85:024116-1–024116-5.
[17] Botti S, Flores-Livas JA, Amsler M, Goedecker S, Marques MAL. Low-energy silicon allotropes with strong absorption in the visible for photovoltaic applications. Phys Rev B. 2012;96:121204-1–121204-5.
[18] Wang Q, Xu B, Sun J, Liu H, Zhao Z, Yu D, Fan C, He J. Direct band gap silicon allotropes. J Am Chem Soc. 2014;136:9826–9829.
[19] Zhao Y-X, Buehler F, Sites JR, Spain IL. New metastable phases of silicon. Solid State Commun. 1986;59(10):679–682.
[20] Minomura S, Drickamer HG. Pressure induced phase transitions in silicon, germanium and some III-V compounds. J Phys Chem Solids. 1962;23(5):451–456.

[21] Gerk AP, Tabor D. Indentation hardness and semiconductor-metal transition of germanium and silicon. Nature. 1978;271:732–733.
[22] Clarke DR, Kroll MC, Kirchner PD, Cook RF, Hockey BJ. Amorphization and conductivity of silicon and germanium induced by indentation. Phys Rev Lett. 1988;60(21):2156–2159.
[23] Kailer A, Nickel KG, Gogotsi YG. Raman microspectroscopy of nanocrystalline and amorphous phases in hardness indentations. J Raman Spectrosc. 1999;30:939–946.
[24] Bradby JE, Williams JS, Swain MV. In situ electrical characterization of phase transformations in Si during indentation. Phys Rev B. 2003;67:085205/1–085205/9.
[25] McMahon MI, Nelmes RJ, Wright NG, Allan DR. Pressure dependence of the Imma phase of silicon. Phys Rev B. 1994;50(2):739–743.
[26] Duclos SJ, Vohra YK, Ruoff AL. Experimental study of the crystal stability and equation of state of Si to 248 GPa. Phys Rev B. 1990;41(17):12012–12028.
[27] Bradby JE, Williams JS, Wong-Leung J, Swain MV, Munroe P. Transmission electron microscopy observation of deformation microstructure under spherical indentation in silicon. Appl Phys Lett. 2000;77(23):3749–3751.
[28] Johnson BC, Haberl B, Bradby JE, McCallum JC, Williams JS. Temperature dependence of Raman scattering from the high-pressure phases of Si induced by indentation. Phys Rev B. 2011;83:235205-1–235205-8.
[29] Ruffell S, Sears K, Bradby JE, Williams JS. Room temperature writing of electrically conductive and insulating zones in silicon by nanoindentation. Appl Phys Lett. 2011;98:052105-1–052105-3.
[30] Rao R, Bradby JE, Williams JS. Patterning of silicon by indentation and chemical etching. Appl Phys Lett. 2007;91:123113/1–123113/3.
[31] Brazhkin VV, Lyapin AG, Popova SV, Voloshin RN. Solid-phase disordering of bulk Ge and Si samples under pressure. Pis'ma Zh Eksp Teor Fiz. 1992;56(3):152–156.
[32] Ge D. TEM investigation of contact loading induced phase transformation in silicon [Ph.D. thesis]. Philadelphia, PA: Drexel University; 2004.
[33] Wykoff RWG. Crystal structures 1. 2nd ed. New York: Interscience Publishers; 1963.
[34] Downs RT, Hall-Wallace M. The American mineralogist crystal structure database. Am Mineral. 2003;88:247–250.
[35] Aroyo MI, Perez-Mato JM, Orobengoa D, Tasci E, de la Flor G, Kirov A. Crystallography online: Bilbao crystallographic server. Bulg Chem Commun. 2011;43:183–197.
[36] Aroyo MI, Perez-Mato JM, Capillas C, Kroumova E, Ivantchev S, Madariaga G, Kirov A, Wondratschek H. Bilbao crystallographic server i: databases and crystallographic computing programs. Z Krist. 2009;211:15–27.
[37] Aroyo MI, Kirov A, Capillas C, Perez-Mato JM, Wondratschek H. Bilbao crystallographic server ii: representations of crystallographic point groups and space groups. Acta Crystallogr. 2006;A62:115–128.
[38] Microcal Software, Inc. Northampton, MA. Microcal Origin Version 6.0; 1999.
[39] Langford RM, Petford-Long AK. Preparation of transmission electron microscopy cross-section specimens using focused ion beam milling. J Vac Sci Technol A. 2001;19(5):2186–2193.
[40] Boehler R, Hantsetters KD. New anvil designs in diamond-cells. High Press Res. 2003;24:391–396.
[41] Klotz S, Chervin J-C, Munsch P, Marchand GL. Hydrostatic limits of 11 pressure transmitting media. J Phys D: Appl Phys. 2009;42:075413-1–075413-7.
[42] Sinogeikin SV, Rod E, Kenney-Benson C, Shen G. Online remote pressure control systems suited for diamond anvil cells at synchrotron beamlines. Manuscript in preparation for Rev Sci Instrum.
[43] Hammersley AP, Svensson SO, Hanfland M, Fitch AN, Häusermann D. Two-dimensional detector software: from real detector to idealised image or two-theta scan. High Press Res. 1996;17:235–248.
[44] Hammersley AP. FIT2D: an introduction and overview. ESRF Internal Report, ESRF97HA02T. Grenoble: ESRF; 1997.
[45] Mao HK, Xu J, Bell PM. Calibration of the ruby pressure gauge to 800 kbar under quasi-hydrostatic conditions. J Geophys Res: Solid Earth. 1986;91(B5):4673–4676.
[46] Olijnyk H. Raman scattering in metallic Si and Ge up to 50 GPa. Phys Rev Lett. 1992;68(14):2232–2234.
[47] Rekhi S, Dubrovinsky L, Saxena S. Temperature-induced ruby fluorescence shifts up to a pressure of 15 GPa in an externally heated diamond anvil cell. High Temp – High Press. 1999;31:299–305.
[48] Boehler R. High-pressure experiments and the phase diagram of lower mantle and core elements. Rev Geophys. 2000;38:221–245.
[49] Zha C-S, Boehler R, Young DA, Ross M. The argon melting curve to very high pressures. J Chem Phys. 1986;85:1034–1036.
[50] Voronin GA, Pantea C, Zerda TW, Wang L, Zhao Y. In situ x-ray diffraction study of silicon at pressures up to 15.5 GPa and temperatures up to 1073 K. Phys Rev B. 2003;68:020102-1–020102-4.
[51] Zhao Z, Tian F, Dong X, Li Q, Wang Q, Wang H, Zhong X, Xu B, Yu D, He J, Wang HT, Ma Y, Tian Y. Tetragonal allotrope of group 14 elements. J Am Chem Soc. 2012;134(30):2362–12365.
[52] Kobliska RJ, Solin SA, Selders M, Chang RK, Alben R, Thorpe MF, Weaire D. Raman scattering from phonons in polymorphs of Si and Ge. Phys Rev Lett. 1972;29(11):725–728.
[53] Haberl B, Guthrie M, Malone BD, Smith JS, Sinogeikin SV, Cohen ML, Williams JS, Shen G, Bradby JE. Controlled formation of metastable germanium polymorphs. Phys Rev B. 2014;89:144111-1–144111-6.
[54] Imai M, Yaoita K, Katayama Y, Chen J-Q, Tsuji K. Amorphization from the quenched high-pressure phase of silicon and germanium. J Non-Cryst Solids. 1992;150:49–52.
[55] Imai M, Mitamura T, Yaoita K, Tsuji K. Pressure-induced phase transitions of crystalline and amorphous silicon and germanium at low temperatures. High Press Res. 1996;15:167–189.
[56] Johnson BC, Haberl B, Deshmukh S, Malone BD, Cohen ML, McCallum JC, Williams JS, Bradby JE. Evidence for the r8 phase of germanium. Phys Rev Lett. 2013;110:085502-1–085502-5.